



Universiteit
Leiden
The Netherlands

Biological model representation and analysis

Cao, L.

Citation

Cao, L. (2014, November 20). *Biological model representation and analysis*. Retrieved from <https://hdl.handle.net/1887/29754>

Version: Corrected Publisher's Version

License: [Licence agreement concerning inclusion of doctoral thesis in the Institutional Repository of the University of Leiden](#)

Downloaded from: <https://hdl.handle.net/1887/29754>

Note: To cite this publication please use the final published version (if applicable).

Cover Page



Universiteit Leiden



The handle <http://hdl.handle.net/1887/29754> holds various files of this Leiden University dissertation

Author: Cao, Lu

Title: Biological model representation and analysis

Issue Date: 2014-11-20

Chapter 4

Evaluation of Algorithms for Point Cloud Surface Reconstruction through the Analysis of Shape Parameters

Based on:

L. Cao, F.J. Verbeek. Evaluation of algorithms for point cloud surface reconstruction through the analysis of shape parameters. 3D Image Processing (3DIP) and Applications 2012, Proceedings SPIE Vol. 8290, Bellingham, 82900G, 2012

L. Cao, F.J. Verbeek. Analytical evaluation of algorithms for point cloud surface reconstruction using shape features. Journal of Electronic Imaging, 22 (4), 043008, October 2013

Abstract:In computer vision and graphics, reconstruction of a 3D surface from a point cloud is a well-studied research area. As the surface contains information that can be measured, the application of surface reconstruction may be potentially important for applications in bio-imaging. In the past decade, a number of algorithms for surface reconstruction have been developed. Generally speaking, these algorithms can be separated into two categories: explicit representation and implicit approximation. Most of these algorithms have a sound basis in mathematical theory. However, so far, no analytical evaluation between these algorithms has been presented. The straightforward method of evaluation has been by convincing through visual inspection. Therefore, we designed an analytical approach by selecting surface distance, surface area and surface curvature as three major surface descriptors. We evaluate these features in varied conditions. Our ground truth values are obtained from analytical shapes: the sphere, the ellipsoid and the oval. Through evaluation we search for a method that can preserve the surface characteristics best and which is robust in the presence of noise. The results obtained from our experiments indicate that Poisson reconstruction method performs best. This outcome can now be used to produce reliable surface reconstruction of biological models.

4.1 Introduction

The problem of 3D surface reconstruction from a point cloud is widely studied and we consider it as important in the field of geometric modeling and analysis of biological objects (models) that have been acquired by an imaging device; for that matter we are specifically interested in objects at the microscopic scale.

At present, a number of approaches have been introduced to represent a 3D surface. The approaches are generally classified into two categories: explicit representation and implicit approximation. The major explicit representations include parametric surfaces and triangulated surfaces. Parametric surfaces, such as B-splines [He and Qin, 2004; Pfeifle and Seidel, 1996; Pottmann and Leopoldseder, 2003; Sun et al., 2006] and Bezier patches, attempt to represent all shapes with a set of elementary shapes, i.e. super-quadratics, generalized cylinders, parametric patches, etc. These parametric surfaces can be described by only a few parameters. The reconstructed surface is smooth whilst the data set can be non-uniform. There is, however, one major drawback of parametric surfaces, which is that several parametric patches need to be combined to form a closed surface, resulting in seams between the patches.

Another explicit representation is denoted as triangulated surfaces. In this representation, all or most of the points are directly interpolated based on structures from computational geometry, such as Delaunay triangulations [Boissonnat, 1984], alpha shapes [Amenta et al., 2000], or Voronoi diagrams [Amenta et al., 1998]. The CRUST method [Amenta et al., 1998] is the first one with a provable reconstruction. The CRUST algorithm exploits the Voronoi diagram of the input-point set to reconstruct the surface. Subsequently, POWER CRUST [Amenta et al., 2001] uses a weighted Voronoi diagram to produce a water-tight surface. This algorithm, however, introduces many extra points in the output and also does not produce a triangulated surface. As an improvement to CRUST, theoretical as well as practical, the COCONE algorithm [Amenta et al., 2000] was introduced. In time this was followed by SUPER COCONE [Dey et al., 2001], TIGHT COCONE [Dey and Goswami, 2003] and ROBUST COCONE [Dey and Goswami, 2004]. Triangulated methods have a profound basis in theory and thereby a guaranteed solution, nevertheless, the implicit interpolations have a

negative effect on the sensitivity to noise. Consequently, in order to produce smooth surfaces from noisy data [Kolluri et al., 2004; Mederos et al., 2005], extensive pre- and/or post-processing is required.

The implicit approximation is based on a scheme which integrates characteristic of each point on the surface into a feature function, a.k.a. the implicit function. The implicit function can be constructed in different ways, such as local fitting, global fitting and combined fitting.

In terms of the local fitting method, Hoppe et al. [Hoppe et al., 1992] reconstructed the surface by locally estimating the implicit function as the signed distance to the tangent plane of the closest point. In a volumetric approach Curless and Levoy [Curless and Levoy, 1996] extended the distance function approach for laser range data, in which they also derive error and tangent plane information. Another approach is to capture the local shape of the surface by adaptively subdividing the space [Ohtake et al., 2003]. Global fitting methods normally use globally supported radial basis functions as the implicit function to reconstruct smooth surfaces [Carr et al., 2003]. Radial basis functions based methods are especially useful for repairing large and irregular holes in an incomplete surface. In these methods serious difficulties are encountered in capturing sharp surface features. In combined fitting methods the advantages from both global and local fitting schemes are integrated. In a Fourier-based reconstruction scheme [Kazhdan, 2005] the Fast Fourier Transform (FFT) is used to derive a characteristic function of the solid model. The Poisson reconstruction [Kazhdan et al., 2006a] is associated with the so called ambient space rather than the data points and has a simple hierarchical structure that results in a sparse, well-conditioned system. The implicit function is derived from a Poisson equation, computing a scalar function whose Laplacian equals the divergence of the oriented point samples. All the implicit approaches are particularly convenient since they all guarantee a, so called, watertight 2-manifold surface approximation [Dey and Goswami, 2003]. A large volume of research papers is available on methods for surface reconstruction from a point cloud. A great deal of effort has been put into method design. The existence of such large number of methods makes a systematic evaluation necessary. Although error estimation is available for several methods, the evaluations are still rather inefficiently described. In most cases a rather straightforward

4. EVALUATION OF SURFACE RECONSTRUCTION ALGORITHMS

way of evaluation is based on visual inspection. One of the apparent reasons for the lack of more comprehensive evaluation is probably related to the amount of parameters that have to be analyzed when comparing reconstruction methods.

As indicated, we are particularly interested in applying surface reconstruction methods in the field of biology. In molecular genetics and developmental biology, the analysis of gene expression is important and requires the development of new elaborate tools for shape analysis. We are modeling the genetic markup through gene expression in relation to development and shape for the Zebrafish (*Danio rerio*) and the Frog (*Xenopus laevis*) [Verbeek et al., 1999b]; to this end, we study the development of the embryo. A surface is used as a shape descriptor and as a means to project gene expression. As for the features it holds that subtle changes in shape need to be noticed so that phenotypical changes can be understood. Therefore, the surface representation needs to be precise and robust. The source datasets that we use for the reconstruction are derived from microscopy [Verbeek, 1999a]; these are stacks of plan parallel images that are aligned as precise as possible. Surfaces are derived from specific labeled volumes in the 3D image and given the context of the application; we need to preserve these surfaces as precise as possible. Numerous contour-based surface reconstruction algorithms exist [Barequet et al., 2003; Braude et al.; Ekoule et al., 1991; Ganapathy and Dennehy, 1982; Jones and Chen, 1994; Klein et al., 2000], however, the more advanced point-based reconstruction technique will support shape analysis in a better manner and parameterization of the surface provides a good starting point. In the contour-based surface reconstruction these algorithms are increasingly used [Barequet et al., 2003]. In order to assess the surface reconstruction we need develop profound insight in the point-based reconstruction technique; i.e. we need to know which algorithm would preserve the shape characteristics best and with the highest accuracy.

In order to complete an analysis of the point bases surface reconstruction algorithms, we have selected four representative algorithms from two major classes. The quality of the surface created by the different algorithms is assessed under noise conditions and compared to known analytical values. In this paper, the point cloud models that we utilized are the sphere, the ellipsoid and the oval; these shapes resemble the early embryo and therefore are realistic as a model.

The evaluation is performed with four methods and for our experiment some related parameters will be selected in the methods evaluation. Given the number of parameters that will be assessed in the evaluation, it should be clear that this evaluation approach requires large memory resources and considerable computation time.

The remainder of this paper is organized follows. In section 4.2, we introduce and propose our evaluation methods. In section 4.3, the experimental results are presented. Finally, in section 4.4, we present our conclusions and indicate directions for our future research.

4.2 Evaluation design

In this paper, we aim at obtaining a higher level of understanding of the major reconstruction approaches currently available. To that end we have selected four representative surface reconstruction methods. Two methods are typical to the group of explicit representation, i.e. Power Crust and Robust Cocone. Two other methods are typical to the group of implicit representation and derive a surface from an implicit approximation, i.e. Fourier-based reconstruction and Poisson reconstruction. According a visual evaluation presented by Kazhdan et al.[Verbeek et al., 1999b] the latter two implicit methods perform best.

In order to make an objective assessment of the quality we will use an error estimation of surface distance, surface area and surface curvature in a comparison of the surface that results from the reconstruction to analytical descriptions of the shape. These three major characteristics of the surface are chosen because: (1) surface distance provides volumetric information of the model which is known as an important global Riemannian invariant, (2) surface area represents the shape of the surface which is a notable integral property, and (3) surface curvature is one of the critical intrinsic properties for providing information on the local shape of a surface. These three features are the paramount ones providing the geometric information of the surface model. A sound error estimation based on these three features would present us a good and objective impression of the performance of each of the surface reconstruction methods.

The point cloud models used in the evaluation are three synthetic objects i.e. the sphere, the ellipsoid and the oval. The reason for employing synthetically generated objects is that we can compute the surface area and surface curvature from the parametrical mathematical representation of these synthetic surfaces. Furthermore, it is also convenient for the calculation of surface distance between synthetic objects and reconstructed objects. Moreover, the biological models that we intend to reconstruct also portray these spherical or elliptical surface characteristics. Thus, this analytical approach supports a more thorough understanding the behavior of different reconstruction methods in the context of the intended application.

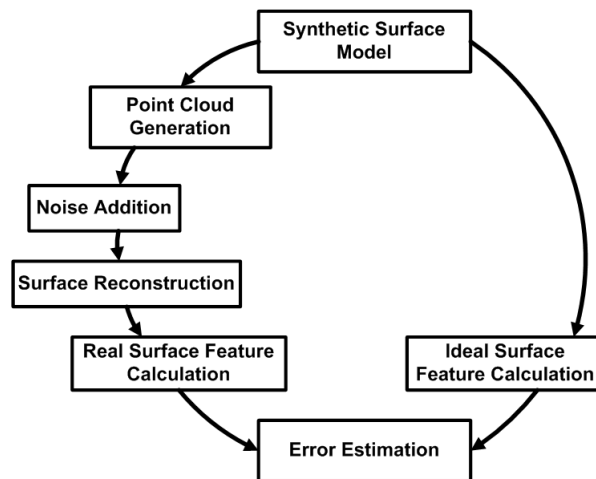


Figure 4.1. Evaluation Design Workflow.

4.2.1 Generation of points and noise

According to our observations, surface curvature differs with point location of the point on the surface, e.g. the surface curvature on the sphere is always equal while the curvature on the ellipsoid changes with spatial location. Therefore, we generate point samples for the synthetic objects in accordance with the surface curvature, so as to properly preserve the surface characteristics. For the sphere, the best way to represent its curvature is generating the surface sample points with a uniform distribution. For the ellipsoid, we generate the points sample according to the equation:

$$\frac{(x - xc)^2}{xr^2} + \frac{(y - yc)^2}{yr^2} + \frac{(z - zc)^2}{zr^2} = 1, \quad (4.1)$$

Where $[xc,yc,zc]$ represents the center of ellipsoid and xr , yr and zr denotes the equatorial radii (along the x y and z axes). In the case of the oval shape, we use the equation provided by Yamamoto [Solvenus and Yamamoto, 2011]. They treat an oval shape by rotating the oval curve around x axis. The equation of a 3D oval surface is given by the following equations:

$$\begin{cases} x = a \cos \theta \\ y = b \cos\left(\frac{\theta}{4}\right) \sin \theta \cos \phi \\ z = b \cos\left(\frac{\theta}{4}\right) \sin \theta \sin \phi \\ 0 \leq \theta \leq \pi \end{cases} \quad (4.2)$$

where $a = 0.5$, $b = 0.37$, $0 < \phi < 2$. With the coordinates data calculated from Equation 2, we can obtain a nicely distributed point cloud without holes existing on both poles that properly represent the surface curvature characteristic.

For the Fourier-based reconstruction and the Poisson reconstruction methods, the generation of point position as an input is not sufficient. These two methods require an oriented point-set as an input. We, therefore, apply point normal calculation as described by Hoppe et al.[Hoppe et al., 1992].

Uniformly distributed noise is added randomly on the point cloud so as to estimate the robustness of each of the methods in the presence of noise. Most of the methods are robust to the Gaussian noise, e.g. the Fourier-based reconstruction algorithm; we therefore have chosen to observe the performance of these methods using uniformly distributed noise. For this type of evaluation we consider uniformly distributed noise to be valid and meaningful.

4.2.2 Surface area calculation

Unlike the surface area of a sphere, the surface area of a general ellipsoid cannot be expressed exactly by an analytical function. The equation to approximate the surface area of an ellipse is given as:

$$A \approx 4\pi \left(\frac{a^p b^p + a^p c^p + b^p c^p}{3} \right)^{1/p} \quad (4.3)$$

where a and b denote the equatorial radii (along the x and y axes), c denotes the polar radius (along the z -axis) and, according to Knud Thomsen's formula $p \approx 1.6075$.

Since the equation of oval surface can be treated as parametric surface $\vec{r} = \vec{r}(u, v)$, we thereafter make use of the definition for surface area of parametric surface to calculate the oval area. The surface area can be calculated by integrating the length of the normal vector $\vec{r}_u \times \vec{r}_v$ to the surface over the appropriate region D in the parametric uv plane:

$$A(D) = \iint_D |\vec{r}_u \times \vec{r}_v| \, dudv \quad (4.4)$$

We use the surface area equation expressed in terms of the first fundamental form as follows:

$$A(D) = \iint_D \sqrt{EG - F^2} \, dudv \quad (4.5)$$

where $E = \vec{r}_u \cdot \vec{r}_u$, $F = \vec{r}_u \cdot \vec{r}_v$, $G = \vec{r}_v \cdot \vec{r}_v$. The expression under the square root is precisely $|\vec{r}_u \times \vec{r}_v|$, and so it is strictly positive at the regular points.

In order to estimate the error between the ideal value derived from formulas above and the real value calculated from the output model, we also need to calculate the area of the reconstructed surface. Since the output of the surface is a triangulation, we can derive the overall area by summation of all areas of the triangle patches on the surface.

4.2.3 Point distance calculation

With respect to the point distance error evaluation, we compute the distance from the points on the output triangulated surface to the synthetic surface model. It is easy to find the shortest distance from a point in 3D surface to the sphere surface centered at the origin of the coordinate system.

$$D = R_p - R_s \quad (4.6)$$

where R_p denotes the distance from point to the origin, and R_s denotes the radius of the sphere. For the ellipsoid the distance calculation is less straightforward. In the literature [Eberly, 2011] algorithms are described to compute the distance from an arbitrary point to an ellipsoid; we have adhered to this approach.

Since oval is a parametric surface, we can treat this specific problem of finding the shortest distance from a point to oval surface as a general one of projecting a point onto a parametric surface. Therefore, we apply the method provided by Shi-min [Hu and Wallner, 2005] to project a point orthogonally onto a surface. This method consists of a geometric second order iteration which converges faster than first order methods and whose sensitivity to the choice of initial values is small.

4.2.4 Surface curvature calculation

With respect to curvature, we estimate the error between ideal and real curvature value:

$$Error_c = \frac{\sum_{i=1}^n ||ideal_c| - |real_c||}{n} \quad (4.7)$$

where $ideal_c$ represents the analytically obtained value and $real_c$ represents the measured value from the point cloud reconstruction. From its remarkable symmetry [Conway and Sloane, 1999], we know that the ideal Gaussian and mean curvatures of sphere model are constant. Therefore, for each point on the sphere, the Gaussian curvature is $K = 1/R^2$ and the mean curvature is $H = 1/R$ where R is the radius of the sphere. As for the point on the ellipsoid surface, the

4. EVALUATION OF SURFACE RECONSTRUCTION ALGORITHMS

Gaussian and mean curvature are derived from equation introduced by Jacobs et al. [Jacobsen et al., 2009]. As we have learned, the oval surface is a parametric type surface. For the parametric surface, the first and second fundamental forms of a surface determine its important differential-geometric invariants: the Gaussian curvature, the mean curvature, and the principal curvatures. So we derive the surface curvature of oval by the equation:

$$K = \frac{LN - M^2}{EG - F^2}, H = \frac{EN - 2FM + GL}{2(EG - F^2)} \quad (4.8)$$

where $E = \vec{r}_u \cdot \vec{r}_u$, $F = \vec{r}_u \cdot \vec{r}_v$, $G = \vec{r}_v \cdot \vec{r}_v$, $L = \vec{r}_{uu} \cdot \vec{n}$, $M = \vec{r}_{uv} \cdot \vec{n}$, $N = \vec{r}_{vv} \cdot \vec{n}$, \vec{n} is a unit normal vector to the parameterized surface at a regular point:

$$\vec{n} = \frac{\vec{r}_u \times \vec{r}_v}{|\vec{r}_u \times \vec{r}_v|} \quad (4.9)$$

Up to a sign, these quantities are independent of the parameterization used. However we only use the absolute value of Gaussian curvature and mean curvature to estimate the curvature error, as a result, these quantities are thoroughly independent during our curvature error estimation.

However, because of the addition of noise, points on the output surface are not necessary still on the original ellipsoid surface. To that end, we first find the nearest point on ellipsoid surface for each point on output surface and then calculate the ideal Gaussian/mean curvature of each point on output surface as that of its nearest point on ellipsoid surface.

A large number of approaches have been proposed for triangulated surface curvature calculation [Magid et al., 2007], some of which give very unpredictable results. In order to estimate the real curvature value of points on the output surface, we choose the paraboloid fitting approach [Sander and Zucker, 1990] which is by far one of the most stable methods in the field of surface curvature calculation.

4.3 Experimental results

We evaluate the four representative algorithms on our synthetic models i.e. a sphere with the radius 0.8004, an ellipsoid ($a=0.5$, $b=0.8547$, $c=1.2$) and an oval ($a=1$, $b=0.78$). In this case, these three synthetic models can be more comparable since they are evaluated with the same volume. First of all we need to establish if the number of points generated for the point cloud provides sufficient information for the reconstruction process. In other words, we need to check if the points sample set results in a situation of oversampling or under-sampling. Subsequently, we take a local observation of each algorithm to check the performance at different noise level. Finally, we have an overall view of all the methods to see which one has the best stability and resilience.

4.3.1 Under/oversampling estimation

For the estimation of the under/oversampling, a number of factors need to be taken into consideration. Scale is one of the important parameters included in both the Fourier-based algorithm and Poisson reconstruction method, though slightly different definitions for scale are used by these methods. Generally speaking, the scale factor is defined as a floating point value that specifies the ratio of diameters between the cube used for reconstruction and the bounding cube of the samples. In this estimation we select two factors i.e. input point number and scale. We applied Fourier-based algorithm on the point cloud representing a sphere model without noise and evaluate the surface distance error.

In Figure 4.3 the result of under/oversampling estimation is depicted. As can be seen, the distance error decreases when the number of input points increases. Moreover, the decay of the distance error is relatively sharp at the beginning while in the end it diminishes, especially in the range of 30000 to 50000 input points the error is almost stable. From these results we conclude that if the input point number is over 30000, then, for the reconstruction methods, the model can be considered oversampled.

4. EVALUATION OF SURFACE RECONSTRUCTION ALGORITHMS

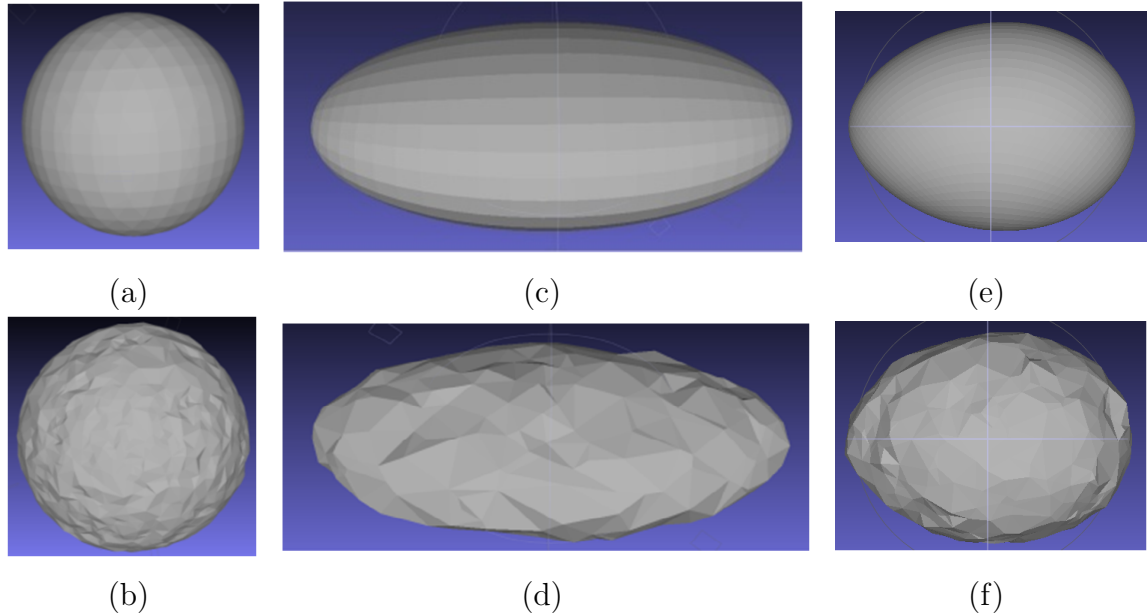


Figure 4.2. Models with and without noise (snapshots from Meshlab [Cignoni, 2010]). (a) Sphere model without noise, (b) Sphere model with noise, (c) Ellipsoid model without noise, (d) Ellipsoid model with noise, (e) Oval model without noise, (f) Oval model with noise.

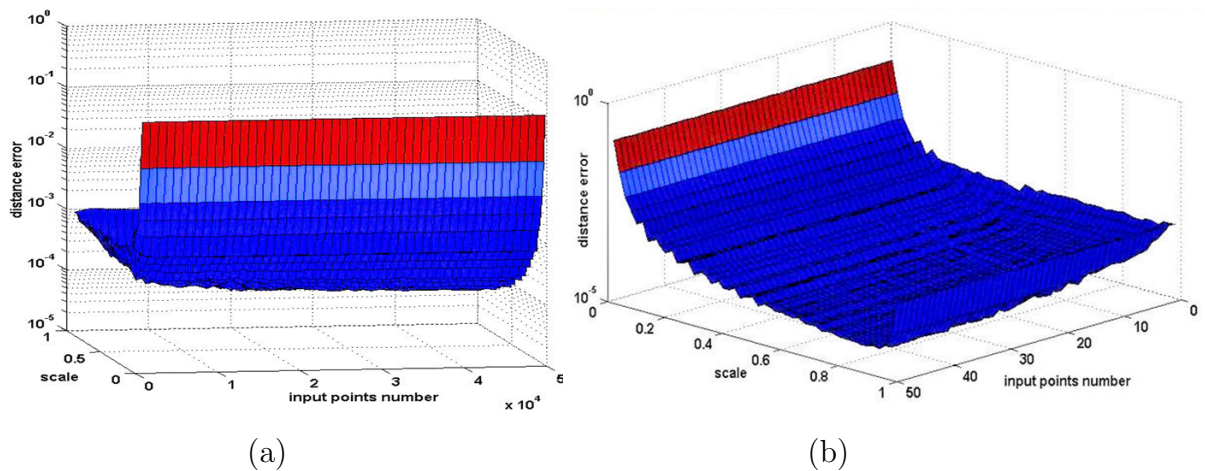


Figure 4.3. Under/oversampling estimation. (a) front view, (b) top view. We apply point distance calculation to estimate the range of the input point number when the model is oversampled. The change of the stripe color from dark blue to red shows the increase of distance error. Therefore, red indicates undersampling.

4.3.2 Local observation

4.3.2.1 Sphere model distance/area error estimation

For convenience of the evaluation procedure, the algorithms are divided into two groups. The first group consists of Power Crust (PC) and Robust Cocone (RCC). By changing the number of input points we observe the performance of two methods under different noise levels. In the reconstruction process we use the default settings of each algorithm. In table 4.1 the changes in the number of output points with respect to the number of input points without the addition noise. Power Crust adds a large number of additional points on the output surface while, for Robust Cocone, the number of output points remains the same. Figure 4.4 (a) and (b) demonstrate that the distance error estimations of these two methods are almost the same. However, in Figure 4.4 (c) and (d) the area error estimation shows clear differences. The area error of Robust Cocone is lower and more stable. Nevertheless, both methods demonstrate the same trend that at increasing levels of noise, the distance error and the area error escalate accordingly.

The second group includes Fourier-based reconstruction (FOU) and Poisson reconstruction (POI) as they have a similar structure of processing and parameters (i.e. resolution, scale). We compare these methods with an oversampling and input of 50000 points; using the same resolution. Their performance is tested within a range of the scale factor and under different levels of noise. In the Fourier-based reconstruction method, as shown in Figure 4.5(a) and 4.5(c), the output number increases together with scale factor. At smaller scales, the error in both parameters is large. This is due to the inadequacy of characteristics integrated in the implicit function since the model only has less than 30 points on the surface, as shown in Figure 4.6(a). When the scale is increasing, the error reduces drastically. An example is shown in Figure 4.6(b). However, at a scale > 0.95 , the error in the area increases again. This is due to the fact that the diameter of the cube used for reconstruction is too small to have any points in the cube. As a result, the output surface model is no longer watertight (i.e. closed) and consequently the area error increases. This is shown in Figure 4.6(c).

In contrast, in the Poisson reconstruction method, the scale setting is the inverse of the scale in Fourier-based reconstruction. As can be seen in Figure 4.5(b) and

4. EVALUATION OF SURFACE RECONSTRUCTION ALGORITHMS

4.5(d); i.e. when the scale increases, the error increases. Although the Poisson error estimation curves are not smooth, the error ranges for both measurements remain relatively small compared to Fourier-based reconstruction method.

Table 4.1. Output points comparison

IP	500	1000	1500	2000	2500	3000	3500	4000	4500	5000	5500
PC	2146	4272	6797	8548	11261	13588	15266	18049	20184	22209	25483
RCC	500	1000	1500	2000	2500	3000	3500	4000	4500	5000	5500

IP=input points, PC= Power Crust output points,
RCC=Robust Cocone output points

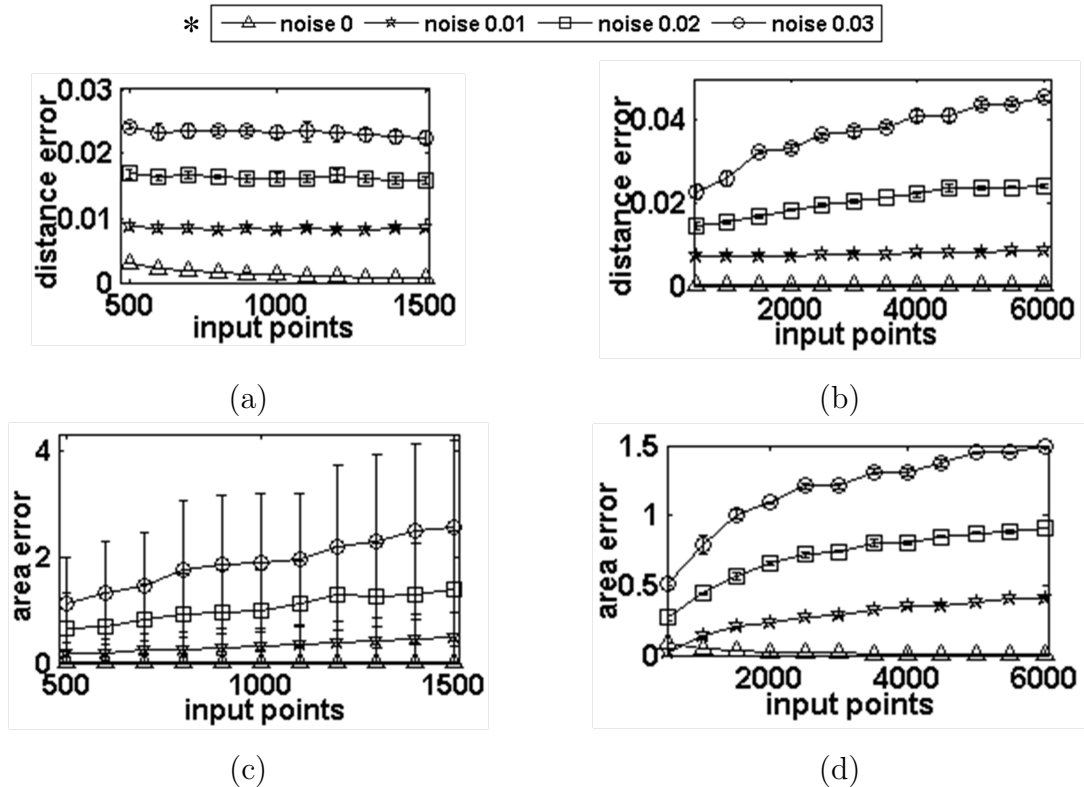


Figure 4.4. Sphere PC/RCC distance and area error estimation. (a) PC Distance error, (b) RCC Distance error, (c) PC Area error, (d) RCC Area error.

* the ranges of the noise and the glyphs used in the graphs in (a-d).

4. EVALUATION OF SURFACE RECONSTRUCTION ALGORITHMS

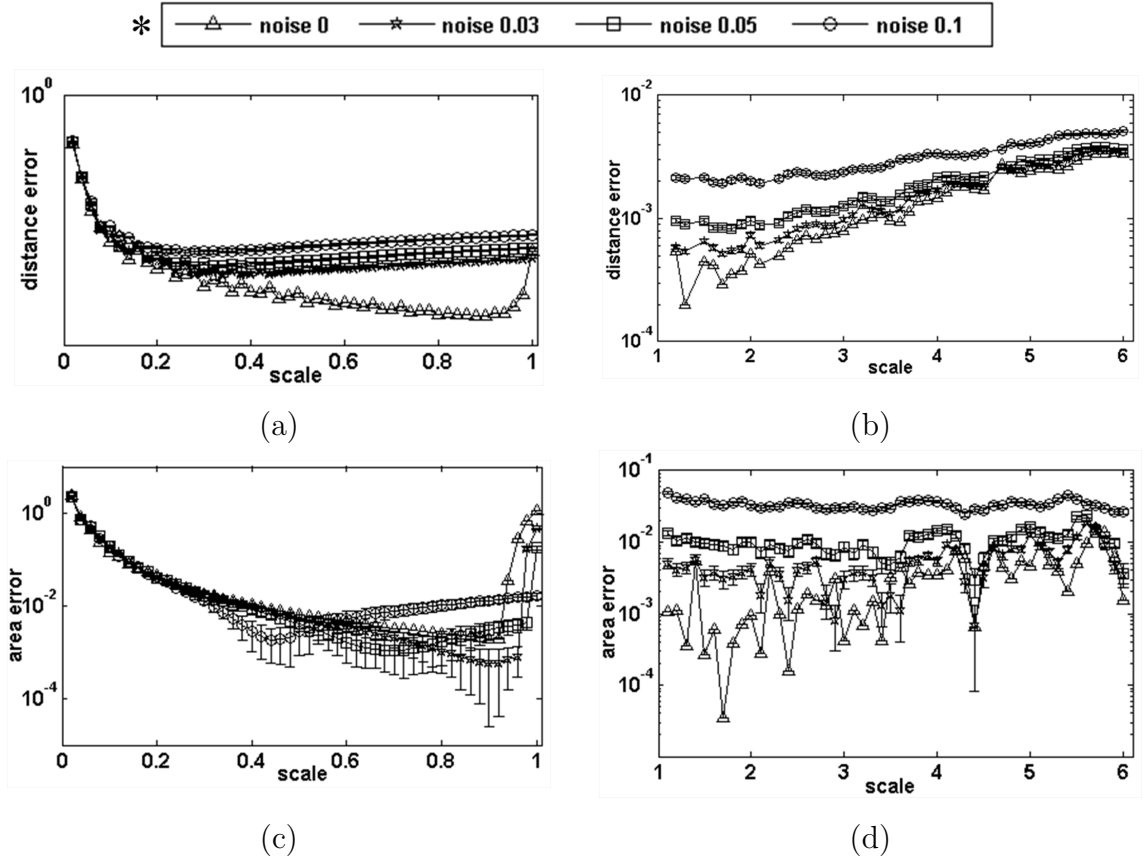
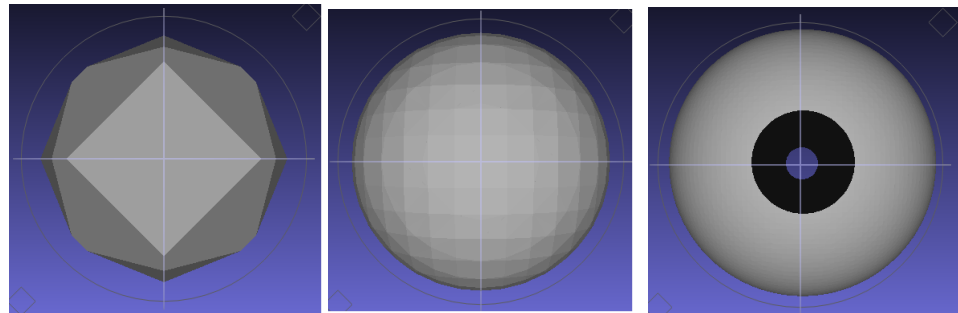


Figure 4.5. Sphere FOU/POI distance and area error estimation. (a) FOU Distance error, (b) POI Distance error, (c) FOU Area error (d) POI Area error.

* the ranges of the noise and the glyphs used in the graphs in (a-d).



(a)

(b)

(c)

Figure 4.6. Sphere output samples of Fourier-based reconstruction method (snapshot in Meshlab [Cignoni, 2010]).(a) sphere output model with scale 0.04, (b) sphere output model with scale 0.2, (c) sphere output model with scale 0.98.

4.3.2.2 Ellipsoid model distance/area error estimation

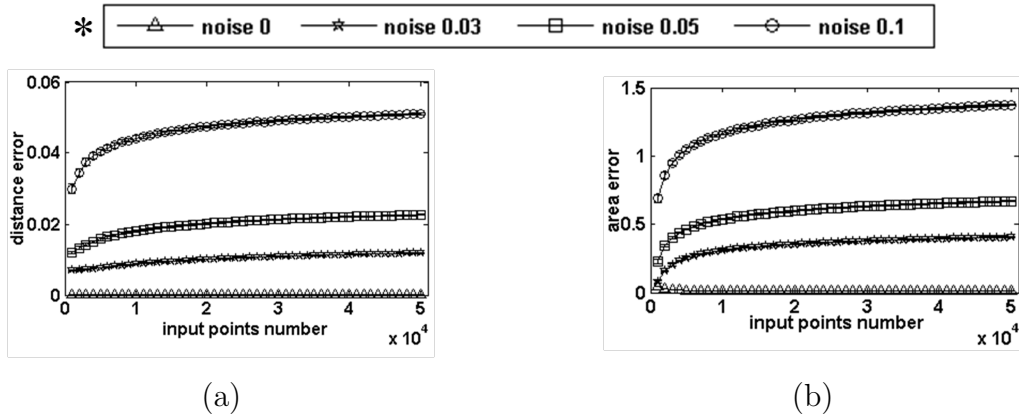


Figure 4.7. Ellipsoid RCC distance and area error estimation (a)RCC Distance error, (b)RCC Area error. * the ranges of the noise and the glyphs used in the graphs in (a-b).

From this part of the evaluation we exclude Power Crust reconstruction methods since the output model is easily broken and obviously not resilient to noise. The remaining three methods are used for further evaluation. Figure 4.7 and Figure 4.8 provide the distance and area evaluations for these three methods. It is clear that the error in distance and area demonstrate the same trend. For example, when the scale factor in Poisson reconstruction increases, both the distance and area error increase as shown in Figure 4.8(c) and 4.8(d). Interestingly, for the results of both Fourier-based and Poisson reconstruction there usually exists an optimum for the minimal distance and area error.

4.3.2.3 Oval model distance/area error estimation

For the oval model, most of the graphs show the same trend as the sphere model and the ellipsoid model. However, in Figure 4.10(d), the area error for Poisson reconstruction method demonstrates some difference. When the noise increases, the area error shows high up at a low scale level. That is because, for a more complicated model, the Poisson reconstruction method integrates more noise points as a feature factor into the characteristic function. As a result the output surface

4. EVALUATION OF SURFACE RECONSTRUCTION ALGORITHMS

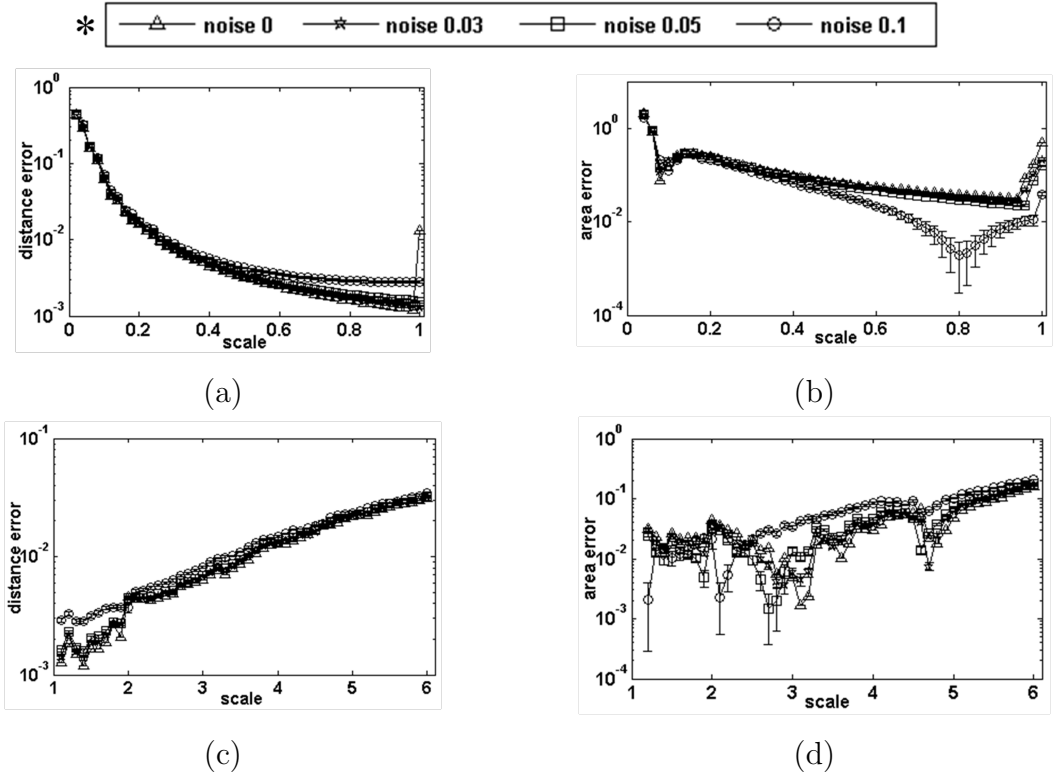


Figure 4.8. Ellipsoid FOU and POI distance and area error estimation. (a) FOU Distance error, (b) FOU Area error, (c) POI Distance error, (d) POI Area error. * the ranges of the noise and the glyphs used in the graphs in (a-d).

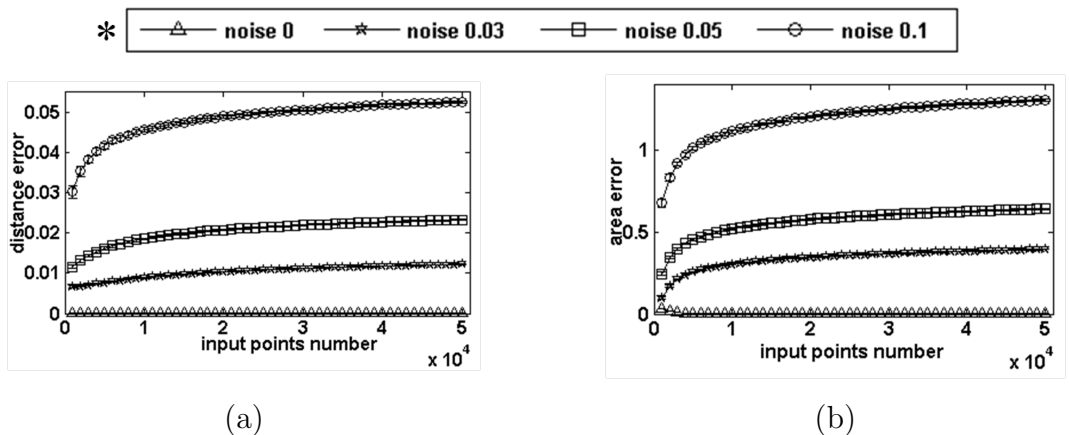


Figure 4.9. Oval RCC distance and area error estimation (a)RCC Distance error, (b)RCC Area error. * the ranges of the noise and the glyphs used in the graphs in (a-b).

4. EVALUATION OF SURFACE RECONSTRUCTION ALGORITHMS

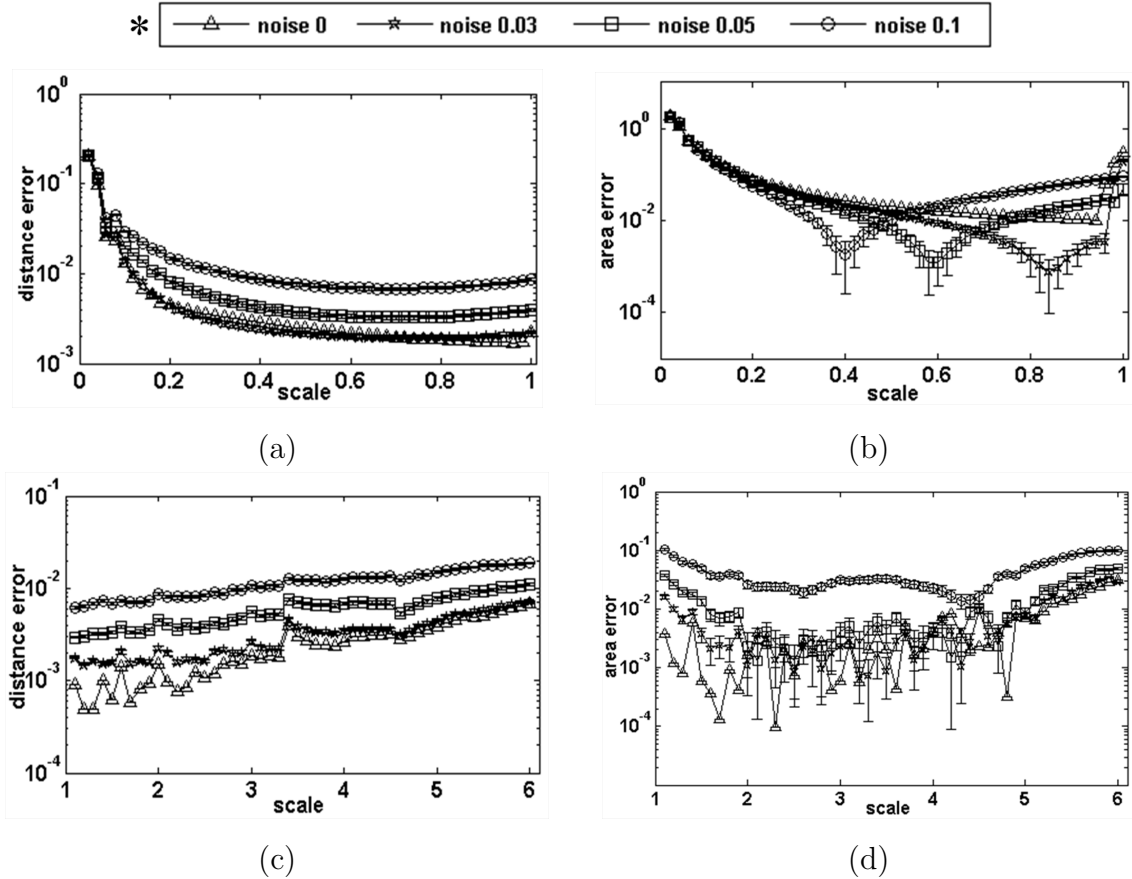


Figure 4.10. Oval FOU and POI distance and area error estimation. (a) FOU Distance error, (b) FOU Area error, (c) POI Distance error, (d) POI Area error.

* the ranges of the noise and the glyphs used in the graphs in (a-d).

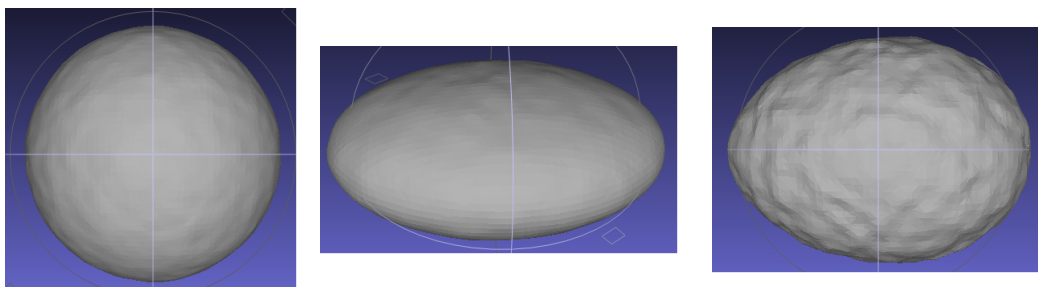


Figure 4.11. Output surface of Poisson reconstruction method with the noise level 0.1 and the scale 1.1 (snapshot in Meshlab [Cignoni, 2010]).

would be rougher and the area error is increasing. In Figure 4.11, we compare the output surface of the sphere, the ellipsoid and the oval from Poisson recon-

struction method with the same noise level and a same low scale setting.

4.3.2.4 Sphere model curvature error estimation

The discussion of curvature error estimation is continued in following three sections. So as to find the reconstruction method that best preserves the curvature characteristic, three methods would be further evaluated. Moreover, in order to obtain a better observation of the results, we use the standard deviation of mean as our error bar for the curvature error estimation sessions.

When we take into a close look at the output surface model from Robust Cocone, we find the orientation of each triangulated surface is not coherent. Moreover, some of the output surface model has non manifold faces. However, for the paraboloid fitting scheme, all the faces on the output surface should be coherently oriented. As a result, we use the script of Meshlab [Lindblad, 2005] software to remove non manifold faces and re-orient all the faces before we estimate the mean/Gaussian curvature. The curvature estimation results from Robust Cocone, as shown in Figure 4.8(a) and 4.8(b), seem irrational. Apart from noise level 0, at increasing noise, the mean/Gaussian curvature error is decreasing. This is caused by the fact that in the reconstruction process of Robust Cocone, at higher levels of noise in the input point cloud, the output number of triangulated points is reduced so as to preserve the smoothness of the output surface. Thus, producing the same number of input points, lower levels of noise generate a surface model with higher resolution resulting in a rougher output surface and a higher local curvature error.

Since with the same scale setting the point number of output surface remains the same, the results of Fourier-based and Poisson reconstruction methods are much more rational. At increasing output resolution, the curvature error decreases at very beginning and increases again at the end. The reason is that, take Fourier-based reconstruction method as an example, when the scale is small the resolution of output surface model is quite low, as shown in Figure 4.6(a). As a result, the local curvature error is high. On the other hand, when the scale is high, more noisy points are preserved. Therefore, the local curvature error is still high. In Figure 4.12 it is illustrated that the Fourier-based and Poisson reconstruction methods have a smaller error in curvature compared to the Robust

4. EVALUATION OF SURFACE RECONSTRUCTION ALGORITHMS

Cocone method.

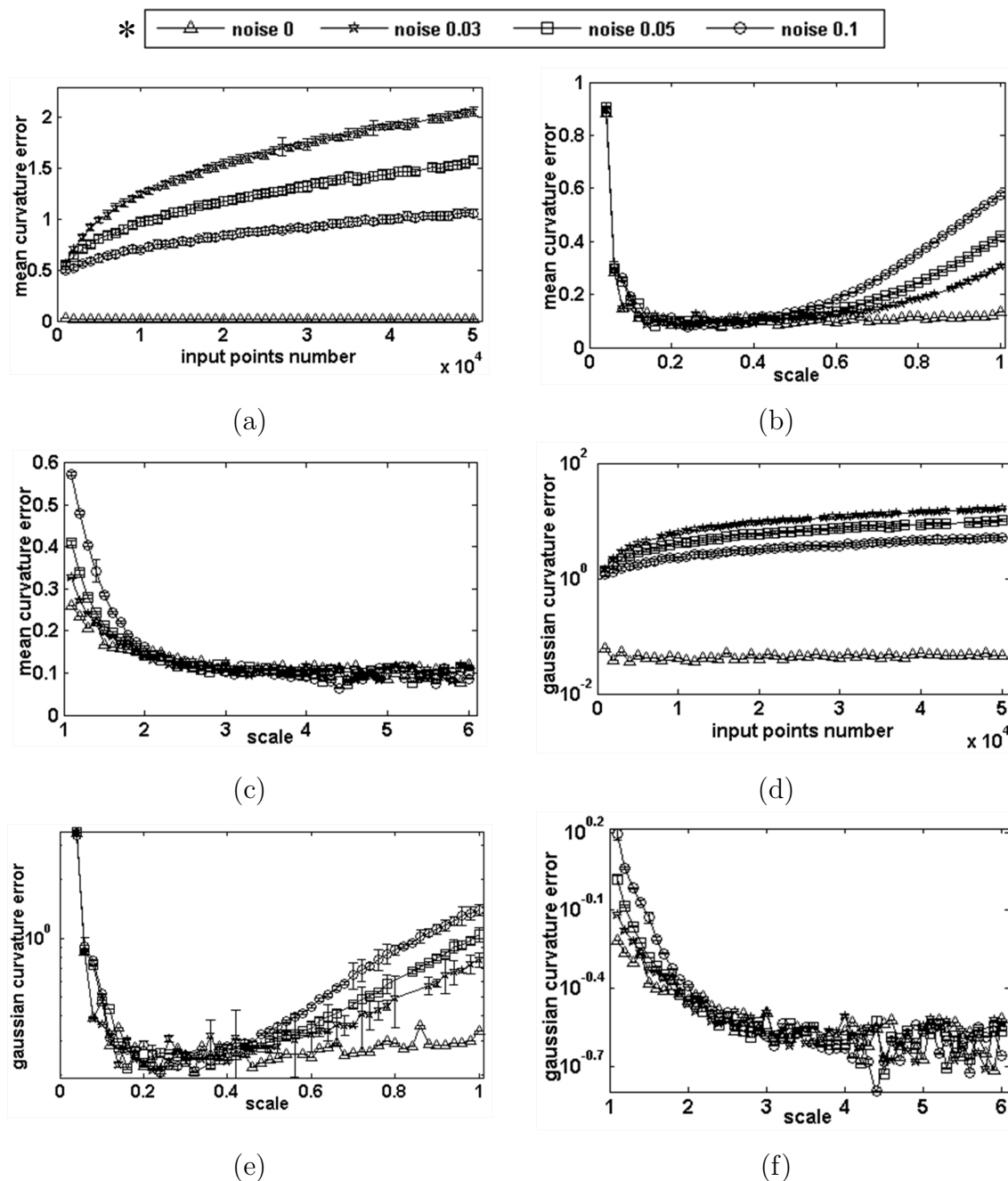


Figure 4.12. Sphere curvature error estimation. (a) RCC Mean curvature, (b) FOU Mean curvature, (c) POI Mean curvature, (d) RCC Gaussian curvature, (e) FOU Gaussian curvature, (f) POI Gaussian curvature. * the ranges of the noise and the glyphs used in the graphs in (a-f).

4.3.2.5 Ellipsoid & oval model curvature error estimation

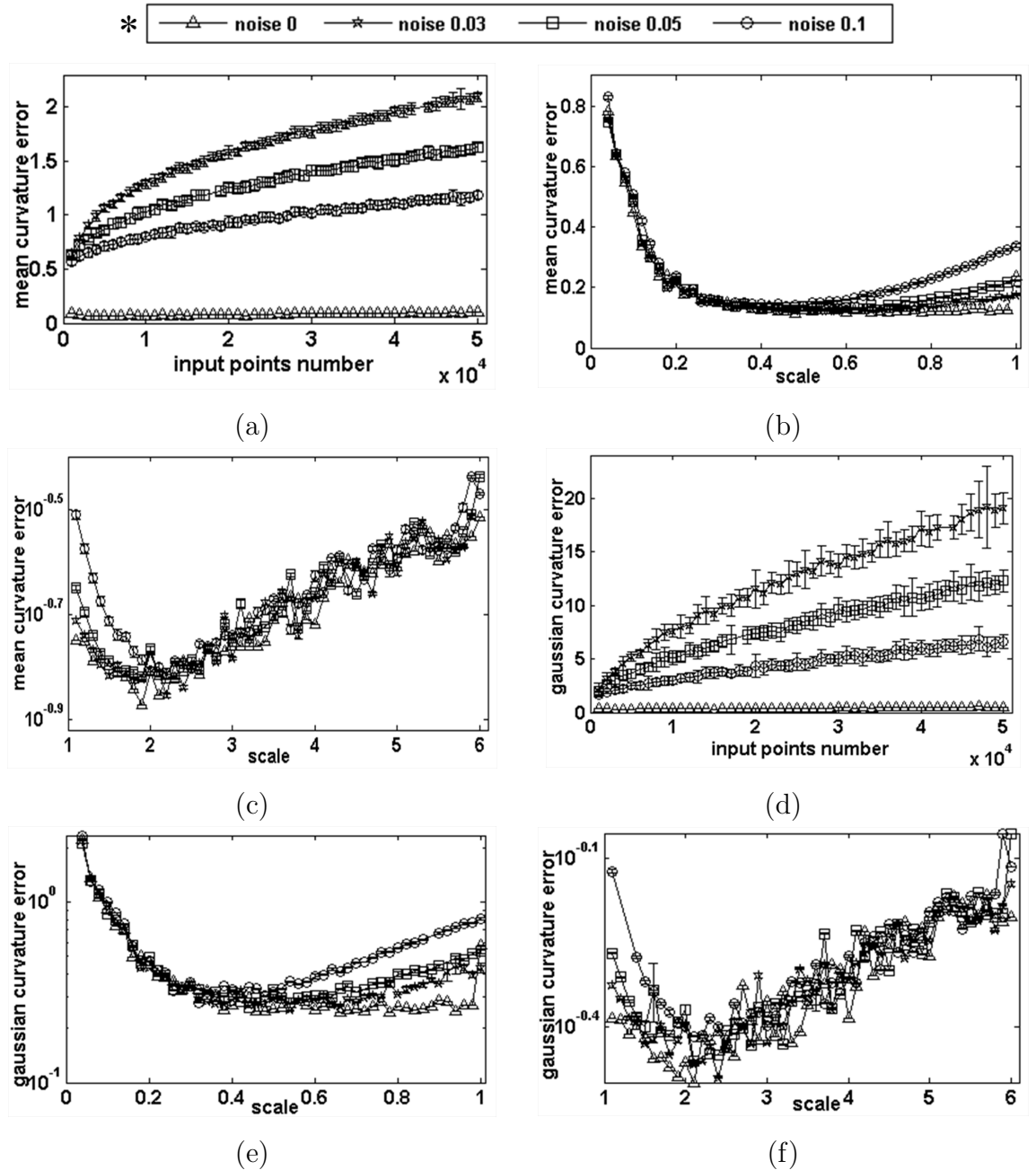


Figure 4.13. Ellipsoid curvature error estimation. (a) RCC Mean curvature, (b) FOU Mean curvature, (c) POI Mean curvature, (d) RCC Gaussian curvature, (e) FOU Gaussian curvature, (f) POI Gaussian curvature. * the ranges of the noise and the glyphs used in the graphs in (a-f).

4. EVALUATION OF SURFACE RECONSTRUCTION ALGORITHMS

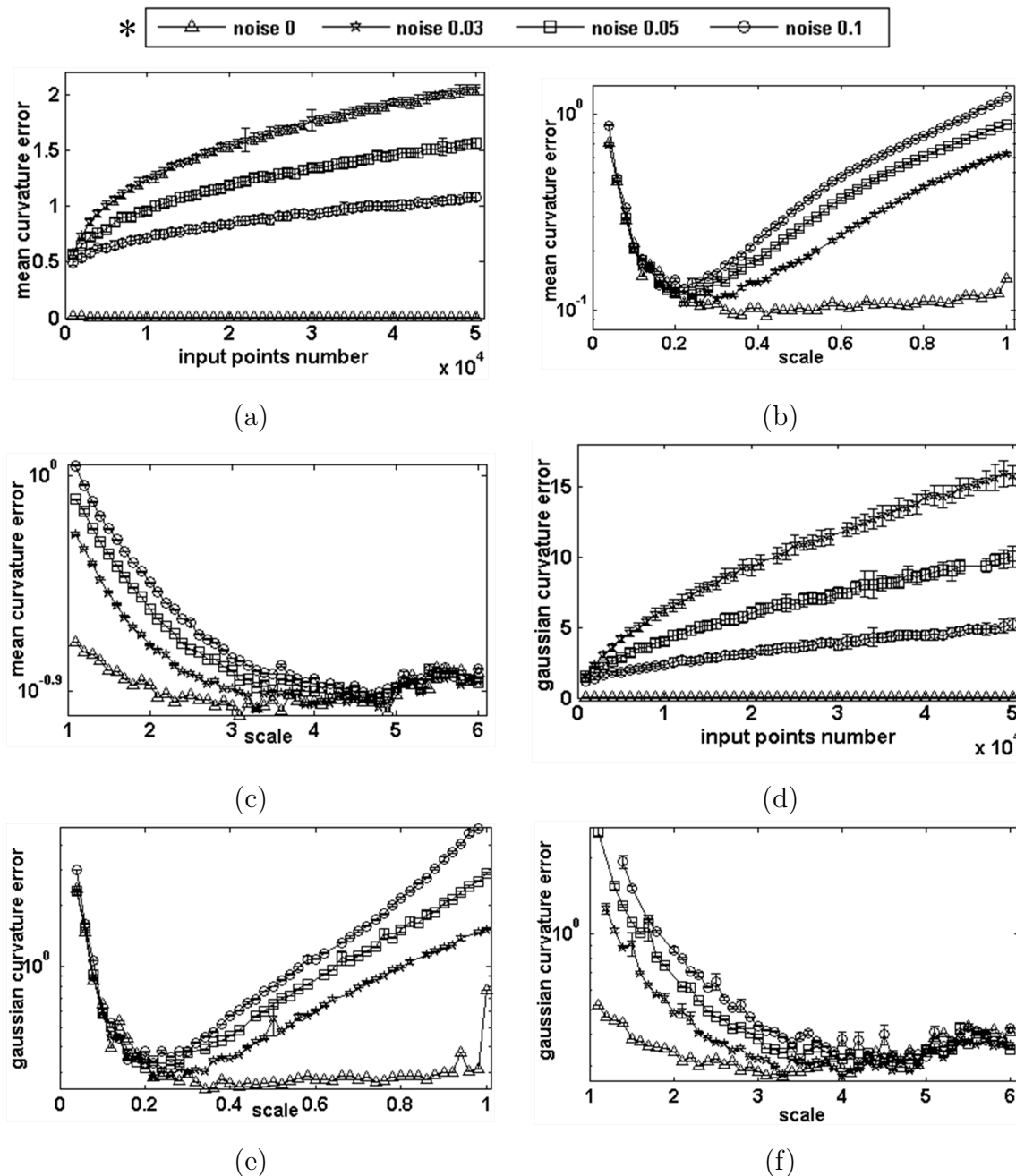


Figure 4.14. Oval curvature error estimation. (a) RCC Mean curvature, (b) FOU Mean curvature, (c) POI Mean curvature, (d) RCC Gaussian curvature, (e) FOU Gaussian curvature, (f) POI Gaussian curvature. * the ranges of the noise and the glyphs used in the graphs in (a-f).

4. EVALUATION OF SURFACE RECONSTRUCTION ALGORITHMS

For the ellipsoid and the oval, the curvature errors show the same trend. In Figure 4.13(a),(b) and Figure 4.14(a),(b), as noise increasing the mean/Gaussian curvature error of Robust Cocone is decreasing. For the Fourier-based and Poisson reconstruction methods the curvature error decreases at very beginning and increases again at the end when the output resolution ascends. Overall the Fourier-based and Poisson reconstruction methods have a smaller error in curvature compared to the Robust Cocone method as shown in Figure 4.13 and Figure 4.14.

4.3.3 Global observation

Table 4.2. Sphere distance/area comparison.

SPHERE	D	A				
	MIN		MEAN		σ	
POI	1.98E-04	0	0.0021	0.0132	0.0012	0.0128
FOU	3.83E-05	9.54E-07	0.0033	0.1092	0.0154	0.3558
RCC	2.23E-07	4.01E-05	0.0199	0.5164	0.0183	0.4334

Table 4.3. Sphere Gaussian/mean curvature comparison.

SPHERE	K	H				
	MIN		MEAN		σ	
POI	0.1516	0.0606	0.3326	0.1322	0.1771	0.0681
FOU	0.1863	0.0725	0.6539	0.1834	11.1527	0.1453
RCC	0.0359	0.0145	5.0525	0.9171	4.5942	0.6271

Table 4.4. Ellipsoid distance/area comparison.

ELLIPSOID	D	A				
	MIN		MEAN		σ	
POI	0.0012	3.81E-06	0.0128	0.05	0.0094	0.0466
FOU	0.0012	4.01E-05	0.0277	0.1578	0.077	0.3011
RCC	7.32E-07	0.0097	0.0193	0.5493	0.0177	0.4615

Table 4.5. Ellipsoid Gaussian/mean curvature comparison.

ELLIPSOID	K	H				
	MIN		MEAN		σ	
POI	0.3169	0.1339	0.5067	0.2142	0.4799	0.0513
FOU	0.2458	0.1153	0.4744	0.2060	0.6649	0.1382
RCC	0.2824	0.0648	6.3863	0.9863	5.7915	0.6215

Table 4.6. Oval distance/area comparison.

OVAL	D	A				
	MIN		MEAN		σ	
POI	4.94E-04	0	0.0059	0.017	0.0043	0.0218
FOU	0.0017	3.81E-06	0.0124	0.1177	0.0318	0.3092
RCC	2.31E-07	1.72E-04	0.0199	0.5263	0.0182	0.4418

4. EVALUATION OF SURFACE RECONSTRUCTION ALGORITHMS

Table 4.7. Oval Gaussian/mean curvature comparison.

OVAL	K	H				
	MIN		MEAN		σ	
POI	0.2637	0.1003	0.5295	0.1939	0.7663	0.1507
FOU	0.2455	0.0935	0.9321	0.3277	1.0066	0.2594
RCC	0.0146	0.0050	5.0815	0.9183	4.5232	0.6306

After an evaluation based on observations in the local ranges, we still need to compare the results as a whole so as to establish the method with the best performance. To that end, we change the input point number from 1000 to 50000 at 1000 point intervals and at the same time change the scale factor in a range of 50 different values. The uniformly distributed noise is added to each set in 4 different levels (cf. Figure 4.8). This procedure has been repeated 50 times for each reconstruction setting. Finally, we calculated the minimum, average and standard deviation for the distance error, the area error, the Gaussian and mean curvature error as estimated from each data set.

Table 4.2 to Table 4.7 present the general evaluation for the combination of all the noise levels. With respect to the sphere model evaluation (Table 4.2 and Table 4.3), Poisson reconstruction method performs more stable (cf. the column). The mean values indicate that Poisson reconstruction still has the best performance with respect to distance error, area error and surface curvature error estimation. For the minimum values, Robust Cocone reconstruction method shows the highest incidence to be in the top. Regarding the Ellipsoid model evaluation (cf. Table 4.4 and Table 4.5), Poisson has the best mean value with relatively high stability in distance error and area error. While Fourier-based reconstruction method has the best mean value in curvature error estimation. However, Poisson always has the lowest standard deviation value. According to the lowest minimum value, Robust Cocone is on top of distance error and mean curvature error evaluation, while Poisson reconstruction method has the lowest minimum value in the area error estimation and Fourier-based reconstruction method has the lowest minimum value in the Gaussian curvature error estimation. As for the oval model (Table 4.6 and Table 4.7), Poisson reconstruction method always has the lowest mean value with the best stability. Robust Cocone has the lowest minimum value of distance error and curvature error estimation, meanwhile, Poisson reconstruction method has the lowest minimum value of area error evaluation.

4.4 Conclusion and future work

In this paper, we have presented an analytical approach to the evaluation of four different methods for 3D surface reconstruction from a point cloud. We generate the point cloud of synthetic geometrical objects i.e. sphere, ellipsoid and oval, and perform error estimation by comparing surface area, distance and curvature between output surface models and ideal synthetic models. By evaluating all parameters of the algorithm and at different noise levels, the total size of the experimental dataset exceeded 50000 files (ply format). From our experimental results we conclude that the Poisson reconstruction method [Kazhdan et al., 2006a] has the most stable performance and is most resilient with increasing amounts of noise in the data. The Fourier-based reconstruction method comes second. Therefore, we can conclude that the class of implicit surface reconstruction methods clearly performs better than the interpolation based class for the surface reconstruction. That is, as we evaluate it to analytical criteria.

The rationale of this work is to obtain a profound assessment of different 3D surface reconstruction approaches, in particular, with respect to measurements that can be derived from reconstructed surfaces. The evaluation will help us in a motivated method selection of surface reconstruction for biological 3D models. For the progress in the research area of bio-imaging and image modelling, such analysis is crucial. With the results surface features for biological shapes can be derived from the data that are obtained by some imaging device, i.e. a microscope. Modern imaging techniques produce 3D images and with the methods described in this paper we can derive surface estimations directly from the image data. In general, these images are pre-processed and sublimated to 3D models. In that case, the methodology will be applied in the same manner; that is, starting from an annotated 3D model [Verbeek, 1999a].

Given a 3D representation, other approaches for surface area computation have been described; early methods use the statistical approach from stereology [Baddeley et al., 1986] to come to an estimation of the surface area. These methods can be very efficient if prior information on the shape can be used; and the stereology approach is still successfully used [Ziegel and Kiderlen, 2010]. Taking a

4. EVALUATION OF SURFACE RECONSTRUCTION ALGORITHMS

sampled volume as the starting point, estimators for digitized surfaces have been developed [Lindblad, 2005; Mullikin and Verbeek, 1993]; these are based on the probability that a certain voxel-position can contribute to the surface area and weights are assigned to surface voxel configurations. Moreover, the estimators on volume data require an isotropically sampled image; this is not in all cases possible. Stereology is able to deal with the non-isotropically sampled data and the undersampling in the z-direction is specifically addressed. The stereology is therefore successfully used with images obtained from physical sections. The method based on implicit surface reconstruction can very well deal with undersampling and therefore it is suitable for models derived from physical sections or otherwise undersampled input.

The methods described in this paper first derive a surface which is subsequently used in the measurements. In this manner the initial sampling is surpassed; the surface description allows extracting a number of features from the surface, i.e. surface area, curvature and others. The analytical shapes that we have used for the assessment of the surface description provide useful information on the surface representations. From tables 4.2-4.7 we learn that the more the shape resembles a sphere, the more accurate the measurement will be. The ovaloid shape is closer to the sphere than the ellipsoid shape and this is reflected in the resulting error measurement. Including previous results [Cao and Verbeek, 2012] we conclude that the error of the shape increases with size. Importantly, with the given shapes the error and the coefficient of variation are below the range that one expects as variation in a measurement of a population of individuals as is common in biology. Therefore the measurements can be used to describe differences between individuals of treated/untreated groups, although in all cases reflection on the outcome remains important. Moreover, the analytical shapes that we have exploited are also representing shapes, or at least partially, as we encounter them in nature. The results can therefore be used to assess the range of the error that can be expected with the reconstruction of a surface of a shape; i.e. it resembles more of a sphere or an ellipsoid.

From the results presented in this paper, it is clear that we intend to further exploit the Poisson reconstruction method. Next, we will specifically utilize the results on biological 3D models so as to improve the quality of the surface rep-

4. EVALUATION OF SURFACE RECONSTRUCTION ALGORITHMS

representations as well as making the surface representations suitable for analytical approaches. The imaging research supporting analytical description of 3D shapes, i.e. embryos in molecular genetics and development, will greatly benefit from the possibilities provided in this study.